Supplemental materials for

Pericyte-targeting prodrug overcomes tumor resistance to vascular disrupting agents

Minfeng Chen, Xueping Lei, Changzheng Shi, Maohua Huang, Xiaobo Li, Baojian Wu, Zhengqiu Li, Weili Han, Bin Du, Jianyang Hu, Qiulin Nie, Weiqian Mai, Nan Ma, Nanhui Xu, Xinyi Zhang, Chunlin Fan, Aihua Hong, Minghan Xia, Liangping Luo, Ande Ma, Hongsheng Li, Qiang Yu, Heru Chen, Dongmei Zhang, Wencai Ye

Corresponding Authors: Wencai Ye, Dongmei Zhang, or Heru Chen, College of Pharmacy, Jinan University, 601 West Huangpu Road, Guangzhou 510632, China. Phone: 86.20.85220004; Email: chywc@aliyun.com (W. Ye); Phone: 86.20.85222653; Email: dmzhang701@foxmail.com (D. Zhang); Phone: 86.20.38375299; Email: thrchen@jnu.edu.cn (H. Chen).

Supplemental methods

Preparation of DAVLBH

Vinblastine sulfate (100 mg, 0.11 mmol) was added to a mixture of hydrazine hydrolysis (80% soln., 6 mL), methanol (6 mL) and DMSO (5 mL). The mixture was stirred under an argon atmosphere at 80 ℃ for 30 h. The cold reaction mixture was poured into water (3 mL), and the aqueous phase was extracted with CH_2Cl_2 (5 mL × 3). The combined organic layers were washed with a saturated NaCl solution (3 mL), dried over Na_2SO_4, and concentrated under reduced pressure. The residue was purified by a flash column chromatography on silica gel ($MeOH/CH_2Cl_2/Et_3N$, 15:1:0.05) to yield DAVLBH as a white powder (67.7 mg, 80% yield). ^{1}H NMR (500 MHz, $CDCl_3$) δ 9.55 (s, 1H), 8.20 (s, 1H), 8.04 (s, 1H), 7.52 (d, J = 7.1 Hz, 1H), 7.26-7.10 (m, 3H), 6.61 (s, 1H), 6.09 (s, 1H), 5.85-5.76 (m, 2H), 4.15 (s, 1H), 4.01-3.87 (m, 3H), 3.78 (s, 3H), 3.71-3.65 (m, 1H), 3.60 (s, 3H), 3.40-3.38 (m, 2H), 3.30 (t, J = 14.5 Hz, 2H), 3.22 (s, 1H), 3.12 (d, J = 12.9 Hz, 2H), 2.85 (br s, 1H), 2.81 (s, 2H), 2.78 (s, 3H), 2.61 (s, 1H), 2.47 (s, 1H), 2.44-2.36 (m, 2H), 2.27 (d, J = 13.7 Hz, 1H), 2.02 (s, 1H), 1.80-1.74 (m, 3H), 1.48 (d, J = 14.0 Hz, 1H), 1.39 (d, J = 13.4 Hz, 1H), 1.35-1.23 (m, 4H), 0.95 (s, 3H), 0.89 (s, 3H). ^{13}C NMR (125 MHz, $CDCl_3$) δ 175.1, 173.9, 158.1, 152.4, 135.0, 131.6, 130.3, 129.5, 123.8, 123.8, 122.5, 122.2, 120.3, 118.8, 118.4, 117.0, 110.5, 93.5, 84.4, 80.6, 73.7, 69.7, 66.7, 64.5, 55.9, 55.8, 55.7, 53.3, 52.4, 50.4, 49.8, 48.4, 45.2, 42.17, 41.7, 38.3, 34.5, 34.4, 33.0, 30.4, 28.9, 8.6, 6.9. HR-ESI-MS *m/z* $[M + H]^+$: 769.4283; calculated for $C_{43}H_{57}N_6O_7$, 769.4283.

Preparation of Z-GP-DAVLBH

N-Carbobenzoxy-glycyl-*L*-proline (53.0 mg, 0.18 mmol) in CH_2Cl_2 (2 mL) was added to benzotriazole-1-yl-oxytripyrrolidinophosphonium hexafluorophosphate (110.4 mg, 0.21 mmol) and *N*,*N*-diisopropylethylamine (0.074 mL, 0.42 mmol). The reaction

mixture was stirred at 0 ℃ for 30 min. DAVLBH (136.0 mg, 0.18 mmol) in CH_2Cl_2 (1 mL) was added to the above mixture, and the reaction was increased to room temperature and stirred for 24 h. The reaction was quenched with a saturated, aqueous NH_4Cl solution (1 mL). The aqueous layer was extracted with CH_2Cl_2 (3 mL × 3). The combined organic layers were dried over Na_2SO_4 and concentrated under reduced pressure. The residue was purified by flash column chromatography on silica gel ($MeOH/CH_2Cl_2/Et_3N$, 15:1:0.05) to yield Z-GP-DAVLBH as a white powder (121.7 mg, 65% yield). ^{1}H NMR (400 MHz, $CDCl_3$) δ 9.76 (s, 1H), 9.16 (s, 1H), 8.06 (s, 1H), 7.52 (d, *J* = 7.8 Hz, 1H), 7.3-7.30 (m, 5H), 7.16-7.07 (m, 3H), 6.57 (s, 1H), 6.28 (s, 1H), 6.08 (s, 1H), 5.77 (dd, *J* = 10.2, 4.0 Hz, 1H), 5.70 (d, *J* = 10.3 Hz, 1H), 5.14 (d, *J* = 12.3 Hz, 1H), 5.05 (t, *J* = 11.7 Hz, 1H), 4.63 (d, *J* = 5.0 Hz, 1H), 4.09-4.06 (m, 2H), 4.00-3.91 (m, 2H), 3.76 (s, 3H), 3.68-3.65 (m, 1H), 3.59-3.57 (m, 3H), 3.38 (d, *J* = 13.7 Hz, 2H), 3.28 (d, *J* = 11.4 Hz, 2H), 3.17 (d, *J* = 5.7 Hz, 1H), 3.11 (d, *J* = 12.8 Hz, 3H), 2.81 (s, 6H), 2.59 (s, 1H), 2.39 (d, *J* = 10.7 Hz, 2H), 2.26 (d, *J* = 11.4 Hz, 2H), 2.13-1.92 (m, 5H), 1.68-1.61 (m, 3H), 1.49-1.43 (m, 1H), 1.41-1.36 (m, 1H), 1.33-1.22 (m, 4H), 0.89 (q, *J* = 7.7 Hz, 6H). ^{13}C NMR (125 MHz, $CDCl_3$) δ 175.2, 171.1, 169.8, 168.8, 158.1, 156.6, 152.8, 136.5, 134.9, 131.6, 130.4, 129.4, 128.4 (2 × C), 127.9, 127.9 (2 × C), 123.9, 123.7, 122.4, 122.1, 120.1, 118.7, 118.4, 116.9, 110.4, 93.6, 83.5, 80.9, 73.7, 69.7, 66.8, 66.5, 64.4, 58.8, 55.8, 55.8, 55.7, 53.2, 52.3, 50.4, 49.8, 48.3, 46.3, 44.8, 43.4, 42.4, 41.6, 38.6, 34.3, 32.8, 30.2, 29.6, 28.8, 28.4, 24.7, 8.5, 6.9. HR-ESI-MS *m/z* $[M + Na]^+$: 1079.5213; calculated for $C_{58}H_{72}N_8O_{11}Na$, 1079.5213.

Preparation of Boc-AP-DAVLBH

Boc-*L*-alanyl-*L*-proline (57.3 mg, 0.20 mmol) in CH_2Cl_2 (2 mL) was added to benzotriazole-1-yl-oxytripyrrolidinophosphonium hexafluorophosphate (156.1 mg,

0.30 mmol) and *N*,*N*-diisopropylethylamine (0.099 mL, 0.60 mmol). The reaction mixture was stirred at 0 ℃ for 30 min. DAVLBH (153.8 mg, 0.20 mmol) in CH_2Cl_2 (1 mL) was added to the above mixture, and the reaction temperature was increased to room temperature and stirred for 24 h. The reaction was quenched with a saturated, aqueous NH_4Cl solution (1 mL). The aqueous layer was extracted with CH_2Cl_2 (3 mL × 3). The combined organic layers were dried over Na_2SO_4 and concentrated under reduced pressure. The residue was purified by preparative HPLC using a reversed-phase C-18 silica gel column (MeOH/H_2O/DEA, 75:25:0.005) to obtain Boc-AP-DAVLBH as a white powder (103.7 mg, 50% yield). ^{1}H NMR (500 MHz, $CDCl_3$) δ 9.77 (s, 1H), 8.03 (s, 1H), 7.52 (d, *J* = 7.9 Hz, 1H), 7.15 (d, *J* = 8.6 Hz, 2H), 7.09 (t, *J* = 7.3 Hz, 1H), 6.59 (s, 1H), 6.07 (s, 1H), 5.83-5.80 (m, 1H), 5.77 (d, *J* = 10.4 Hz, 1H), 5.36 (d, *J* = 8.6 Hz, 1H), 4.68 (d, *J* = 7.8 Hz, 1H), 4.52-4.43 (m, 1H), 4.11 (s, 1H), 3.96 (t, *J* = 14.2 Hz, 1H), 3.77 (s, 3H), 3.68 (t, *J* = 10.6 Hz, 2H), 3.59 (s, 3H), 3.53 (s, 1H), 3.39 (d, *J* = 13.7 Hz, 1H), 3.33-3.27 (m, 2H), 3.22-3.19 (m, 1H), 3.13 (s, 1H), 3.10 (s, 1H), 2.85 (d, *J* = 15.6 Hz, 1H), 2.80 (br s, 5H), 2.73-2.71 (m, 1H), 2.61 (s, 1H), 2.44-2.38 (m, 4H), 2.28 (s, 1H), 2.25 (s, 1H), 2.16-2.10 (m, 2H), 2.04-1.98 (m, 3H), 1.75-1.67 (m, 2H), 1.64 (br s, 1H), 1.43 (s, 9H), 1.34-1.29 (m, 6H), 1.26-1.22 (d, *J* = 8.2 Hz, 2H), 1.15 (t, *J* = 7.1 Hz, 1H), 0.94 (t, *J* = 7.4 Hz, 3H), 0.89 (t, *J* = 7.4 Hz, 3H).^{13}C NMR (125 MHz, $CDCl_3$) δ 174.8, 173.5, 170.5, 168.6, 158.1, 155.2, 152.7, 135.0, 131.7, 130.2, 129.5, 123.9, 123.7, 122.3, 122.2, 120.3, 118.8, 118.5, 116.9, 110.5, 93.6, 83.8, 80.8, 73.7, 69.8, 66.6, 64.5, 58.3, 55.9, 55.8, 55.7, 53.4, 52.4, 50.4, 49.7, 48.4, 47.8, 47.2, 45.0, 42.3, 41.7, 38.4, 34.5, 34.3, 32.9, 30.3, 29.7, 28.9, 28.4 (3 × C), 26.9, 25.1, 18.6, 8.6, 6.9. HR-ESI-MS *m/z* $[M + H]^+$: 1037.5705; calculated for $C_{59}H_{77}N_8O_{11}$, 1037.5706.

Preparation of Z-GP-DAVLBH-BODIPY

BODIPY-ACID was synthesized based on a previous synthetic procedure (1). BODIPY-ACID (5 mg, 0.016 mmol) in 3 mL DMF was stirred, and the coupling reagent DCC (6 mg, 0.03 mmol) was added. Z-GP-DAVLBH (10 mg, 0.01 mmol) was then added to the above solution, and the reaction was stirred at room temperature overnight in the dark. Subsequently, the reaction was quenched by the addition of 3 mL of water and extracted with 2 × 10 mL of ethyl acetate. The organic layers were washed with 2 × 10 mL of brine and dried over anhydrous Na_2SO_4. Upon solvent evaporation *in vacuo*, the residue was purified by flash column ($MeOH/CH_2Cl_2/NH_3{\cdot}H_2O$, 20:1:0.05) to yield the product as a yellow solid (4 mg, 30%). HR-ESI-MS *m/z* $[M + H]^+$: 1347.8795; calculated for $C_{73}H_{87}BF_2N_{10}O_{12}$, 1346.3724.

Supplemental references

1. Gießler K, Griesser H, Göhringer D, Sabirov T, Richert C. Synthesis of 3 '-bodipy-labeled active esters of nucleotides and a chemical primer extension assay on beads. *Eur J Org Chem*. 2010;2010(19):3611-3620.

Supplemental Figures 1-13

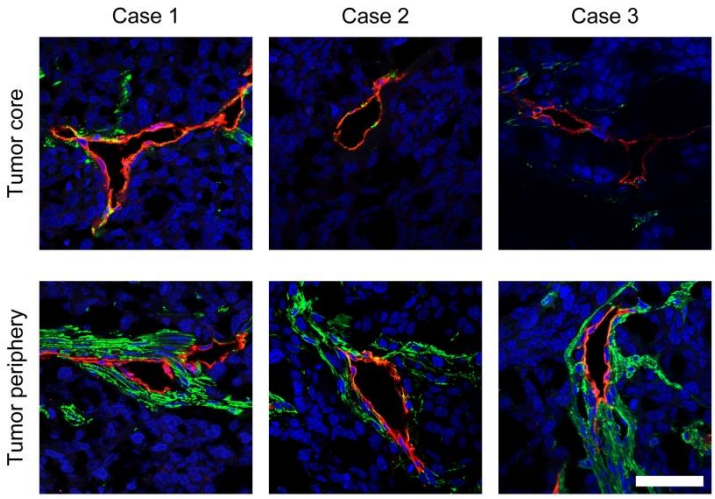

Supplemental Figure 1. Immunofluorescence analysis of pericyte coverage in the tumor core and periphery. MDA-MB-231 tumor xenograft frozen sections were stained with FAPα (green) and CD31 (red) to identify pericytes and ECs, respectively. The images were obtained under confocal microscopy (n = 3). Scale bars, 50 μm.

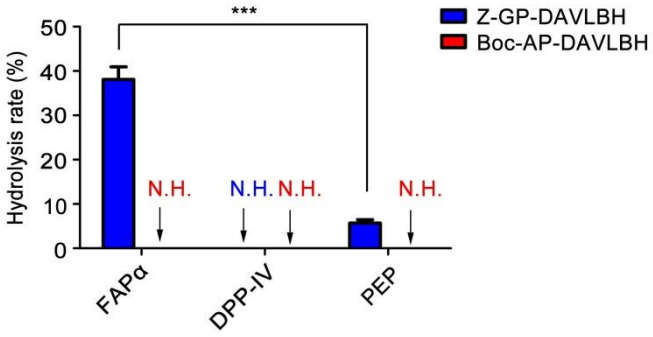

Supplemental Figure 2. Enzymatic efficacy of FAPα, DPP-IV and PEP on Z-GP-DAVLBH and Boc-AP-DAVLBH. Z-GP-DAVLBH was selectively activated by FAPα. Z-GP-DAVLBH (10 μM) was incubated with rhFAPα (5 ng/mL), rhDPP-IV (5 ng/mL) or rhPEP (5 ng/mL) at 37 ℃ for 1 h. Quantification of the hydrolysis rates is shown (n = 3). N.H.: no hydrolysis. The data are expressed as the mean ± SEM. ***$P < 0.001$ (2-tailed unpaired *t* test).

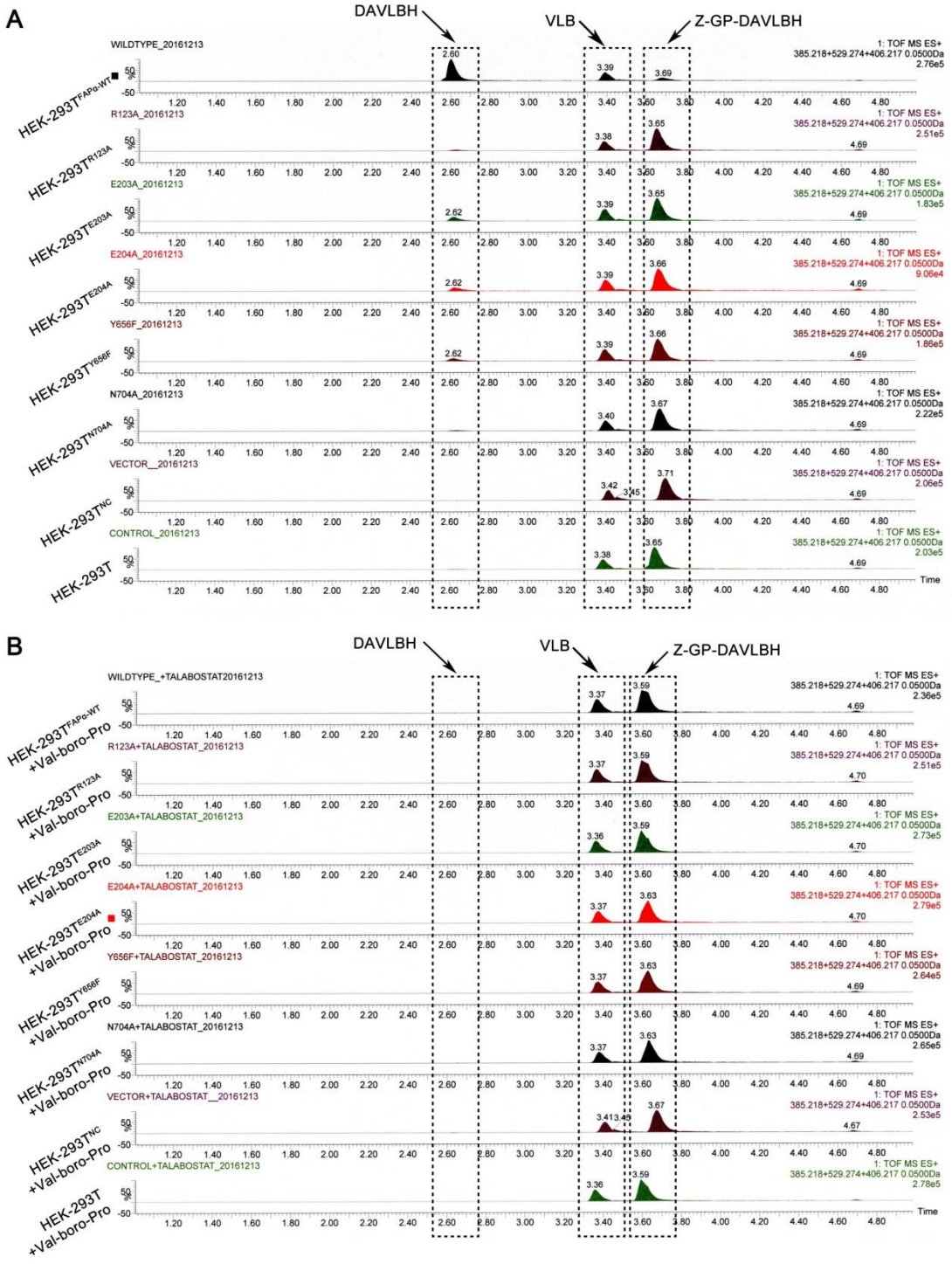

Supplemental Figure 3. Enzymatic efficacy of engineered FAPα-expressing cells on Z-GP-DAVLBH. (A) HEK-293T cells were transiently transfected with vector, wild-type FAPα or mutant FAPα (R123A, E203A, E204A, Y656F, N704A). Z-GP-DAVLBH (10 μM) was incubated with the cells at 37℃ for 2 h, and the

hydrolysis was analyzed by LC/MS. (B) The cells pretreated with 100 μM Val-boro-Pro for 1 h showed negligible hydrolysis on Z-GP-DAVLBH. The representative extracted ion chromatograms are shown. Z-GP-DAVLBH (retention time: ~3.65 min; *m/z* 529.274 $[M+2H]^{2+}$), DAVLBH (retention time: ~2.60 min; *m/z* 385.218 $[M+2H]^{2+}$) and VLB (retention time: ~3.40 min; *m/z* 406.217 $[M+2H]^{2+}$).

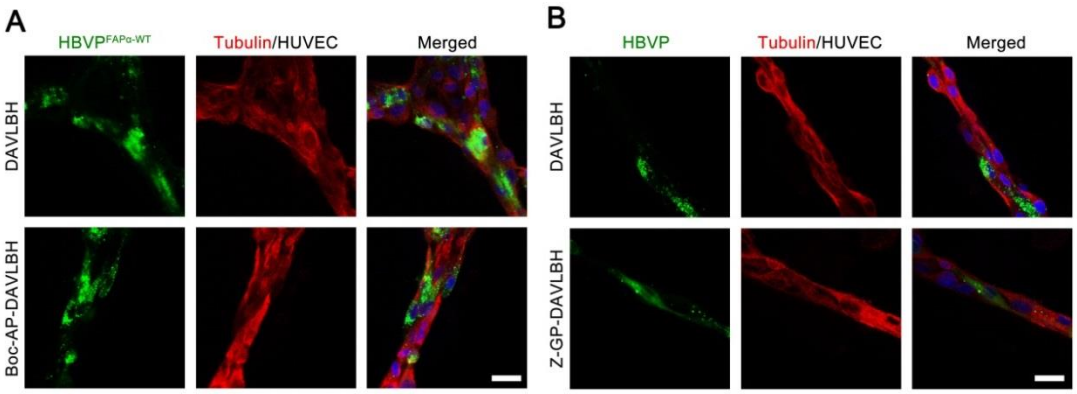

Supplemental Figure 4. Evaluation of the effects of the test compounds on HBVP$^{FAPα-WT}$-HUVEC or HBVP-HUVEC cocultured systems. (**A**) DAVLBH and Boc-AP-DAVLBH have no effects on the β-tubulin (red) cytoskeleton of HBVP$^{FAPα-WT}$ (green, PKH 67 staining) cell coverings on the HUVEC tubes (n = 3). (**B**) DAVLBH and Z-GP-DAVLBH have no effects on the β-tubulin (red) cytoskeleton of HBVP (green, PKH 67 staining) cell coverings on the HUVEC tubes (n = 3). Scale bars, 100 μm.

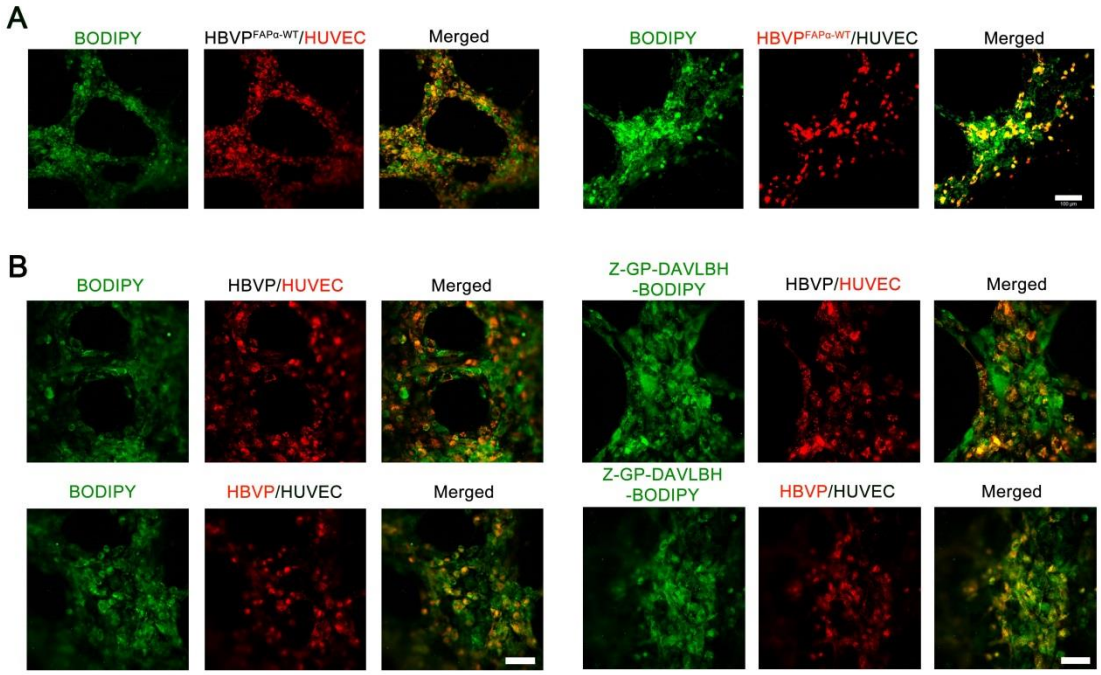

Supplemental Figure 5. Evaluation of the accumulation of BODIPY and Z-GP-DAVLBH-BODIPY in pericyte-endothelial cell cocultured systems. HBVP (red), HBVP$^{FAP\alpha\text{-}WT}$ (red) and HUVEC (red) were stained with PKH 26, respectively. (**A**) Free BODIPY (400 nM) was accumulated non-selectively in HBVP$^{FAP\alpha\text{-}WT}$ and HUVECs in the cocultured system (n = 3). (**B**) Free BODIPY (400 nM) and Z-GP-DAVLBH-BODIPY (400 nM) were accumulated non-selectively in HBVP and HUVECs in the cocultured system (n = 3). Scale bars, 100 μm.

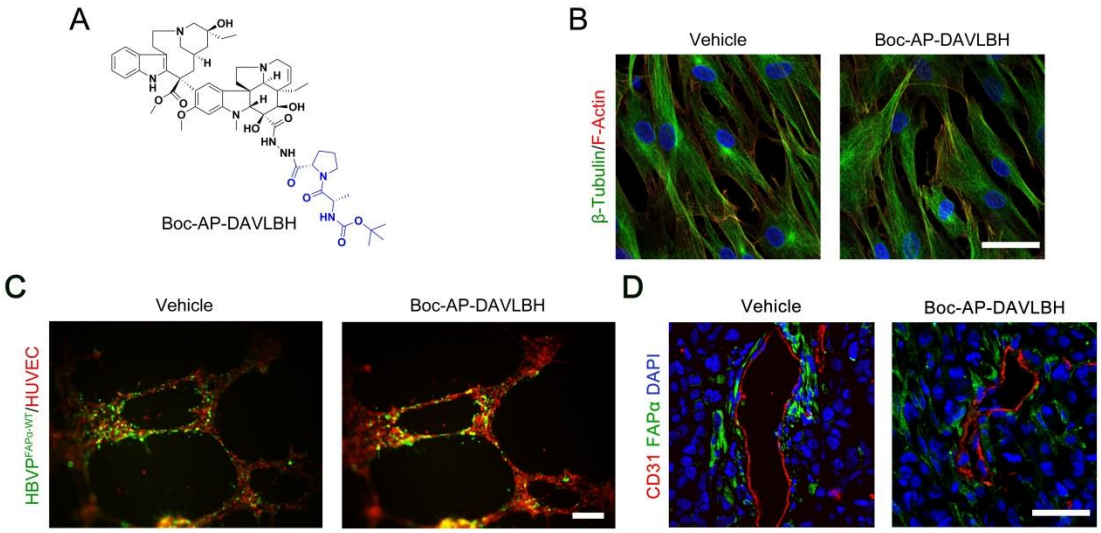

Supplemental Figure 6. Evaluation of the effects of the non-FAPα-activated prodrug Boc-AP-DAVLBH in vitro and in vivo. (**A**) Structure of Boc-AP-DAVLBH. (**B**) Boc-AP-DAVLBH has no effects on the β-tubulin cytoskeleton of HBVP$^{FAPα\text{-}WT}$ (n = 3). Scale bar, 50 μm. (**C**) Boc-AP-DAVLBH has no effects on the HBVP$^{FAPα\text{-}WT}$/HUVEC cocultured tubes (n = 3). HBVP$^{FAPα\text{-}WT}$ (green) and HUVEC (red) were labeled with PKH 67 and PKH 26, respectively. Scale bar, 100 μm. (**D**) Boc-AP-DAVLBH has no effects on tumor vessels in MDA-MB-231 xenografts (n = 5). Tumor tissues were harvested 4 h after i.v. injection of Boc-AP-DAVLBH at 2.0 μmol/kg. Scale bar, 50 μm.

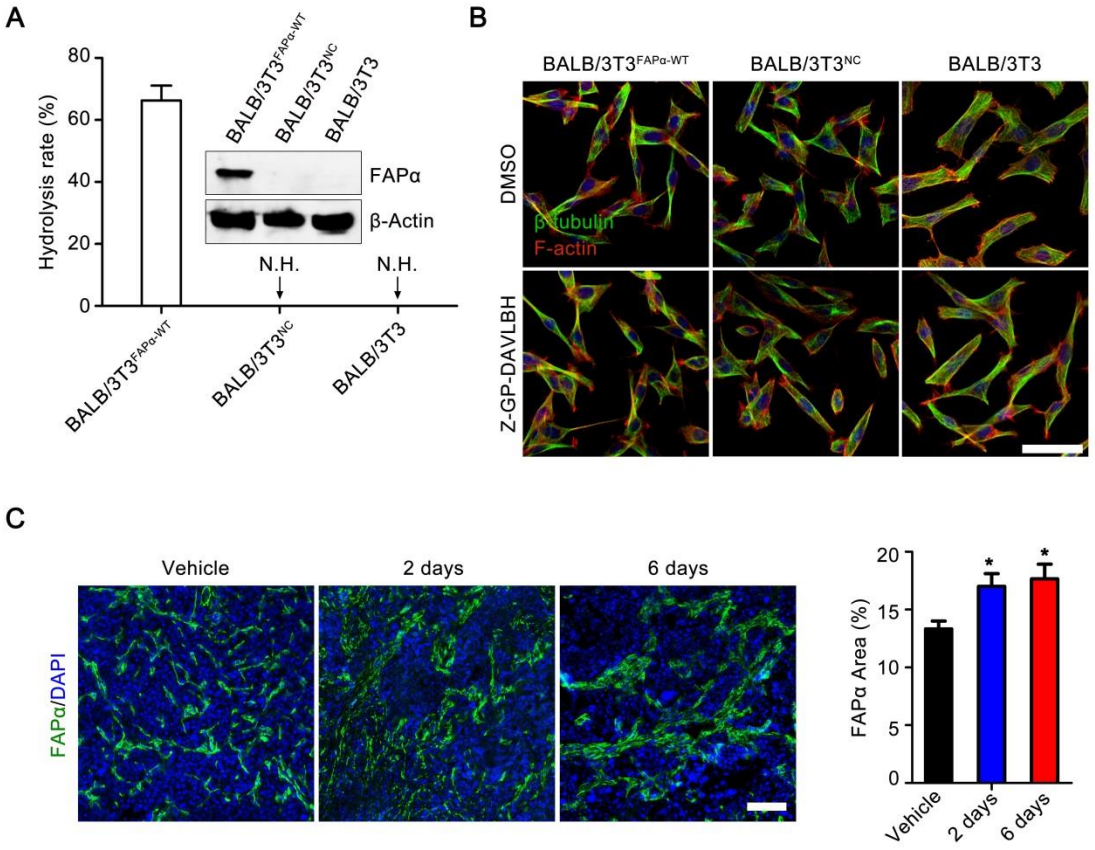

Supplemental Figure 7. Z-GP-DAVLBH has negligible effect on FAPα-expressing cancer-associated fibroblasts. (A) The enzymatic ability of the cells mimicking cancer-associated fibroblasts (BALB/3T3$^{FAPα\text{-}WT}$) on Z-GP-DAVLBH. Quantification of the hydrolysis rate is shown (n = 3). (**B**) The effects of Z-GP-DAVLBH on the β-tubulin cytoskeleton of BALB/3T3$^{FAPα\text{-}WT}$, BALB/3T3^{NC} and BALB/3T3 cells (n = 3). The cells were incubated with 25 nM Z-GP-DAVLBH for 30 min, and β-tubulin (green) and F-actin (red) were observed with a confocal microscope. Scale bars, 50 μm. (**C**) Immunofluorescence analysis of the changes in FAPα staining tumor fibroblasts. Three images were taken per tumor. Quantification of the FAPα area is shown (n = 5). Mice bearing MDA-MB-231 tumor xenografts were received i.v. injection of 2.0 μmol/kg Z-GP-DAVLBH. Four hours later, tumors were obtained and stained for FAPα. Scale bars, 50 μm. The data are expressed as mean ± SEM. *P < 0.05 *versus* vehicle group (1-way ANOVA with Tukey's *post hoc* comparison).

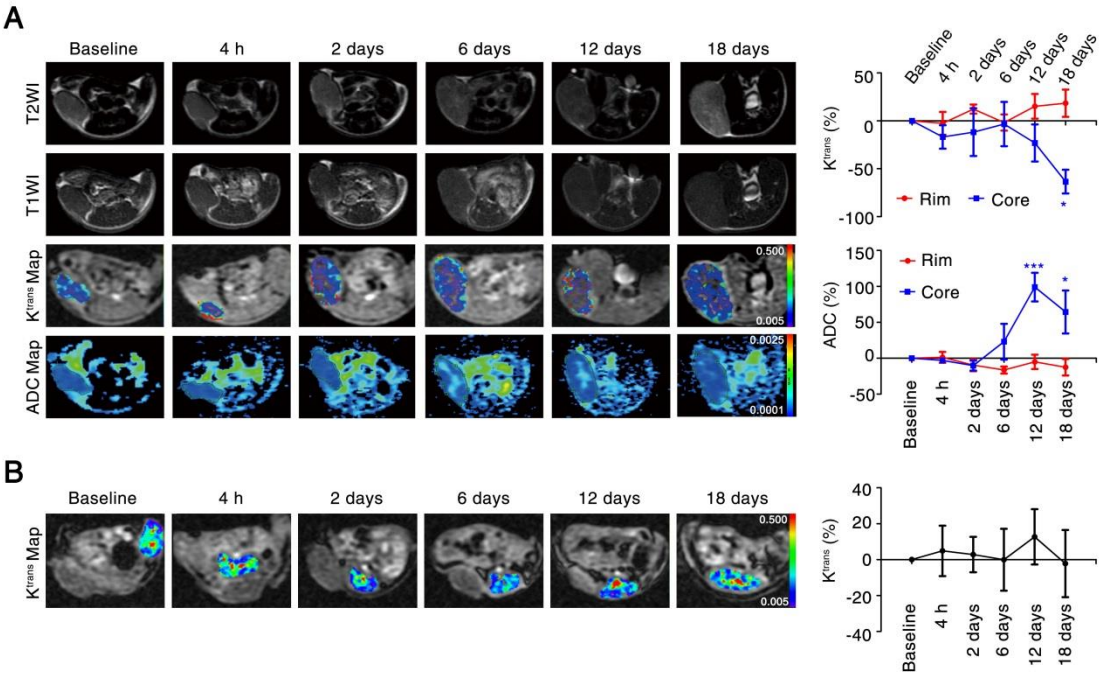

Supplemental Figure 8. MRI monitoring of the vascular disruption effects on MDA-MB-231 xenografts. (**A**) MR images of tumors in the vehicle group (left). Quantification of K^{trans} and ADC values is shown (right, n = 5 mice per group). The mice bearing MDA-MB-231 xenografts received i.v. injection of saline containing 1% DMSO once every two days. The reduction of K^{trans} and the increase in ADC values in the tumor core were resulted from central tumor necrosis caused by tumor development. (**B**) Z-GP-DAVLBH has no significant effect on the K^{trans} values in normal muscle tissues. Quantification of the K^{trans} values is shown (right, n = 5). The K^{trans} values were calculated from the mice bearing MDA-MB-231 xenografts that received i.v. injection of Z-GP-DAVLBH (2.0 μmol/kg) once every two days. The error bar represents the SEM. **P* < 0.05, ****P* < 0.001 *versus* Baseline group (1-way ANOVA with Tukey's *post hoc* comparison).

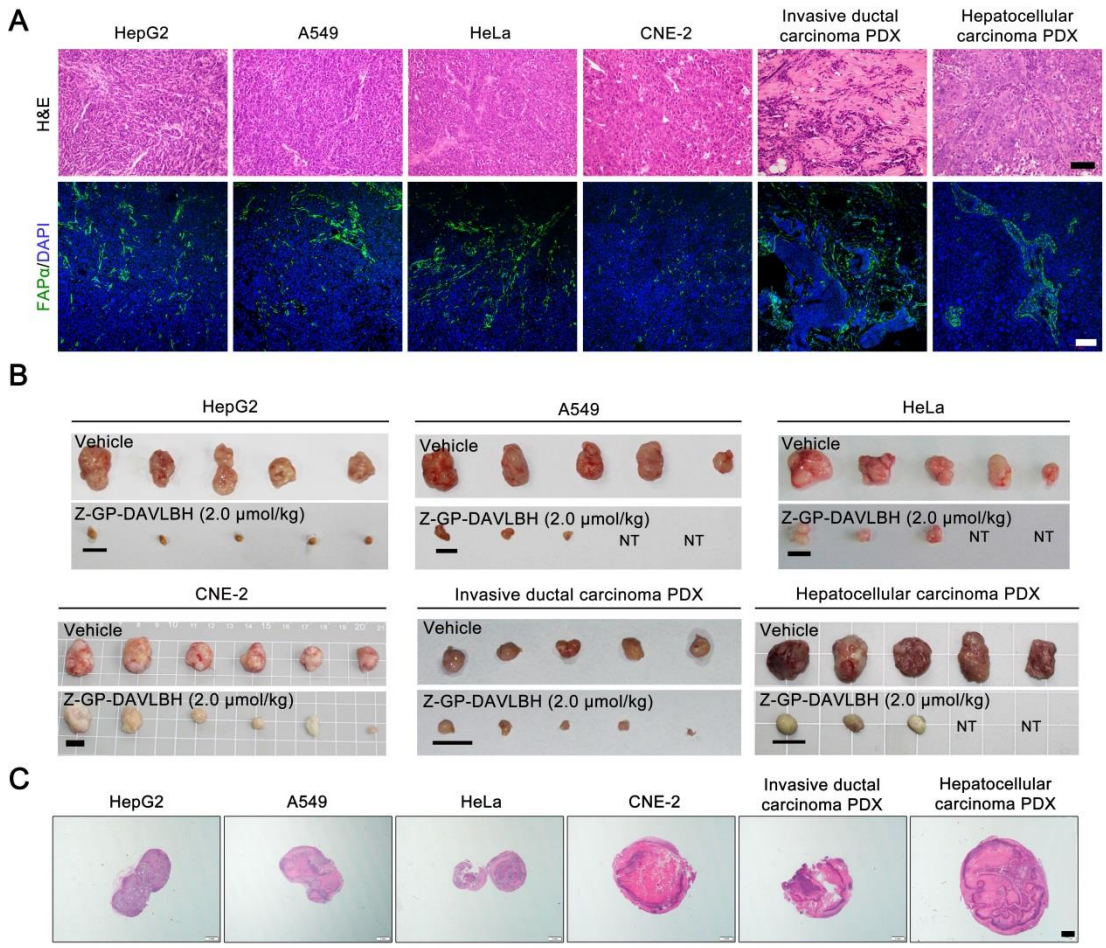

Supplemental Figure 9. Z-GP-DAVLBH has abroad spectrum of antitumor activity. (**A**) H&E and immunofluorescence staining of tumor tissues show FAPα is overexpressed in A549, HeLa and CNE-2 xenografts, as well as primary invasive ductal carcinoma patient-derived xenografts (PDX) and primary hepatocellular carcinoma PDX tumor tissues, thus providing the rationale for using these models to evaluate the antitumor efficacy of Z-GP-DAVLBH. Scale bar, 100 μm. (**B**) Representative images of excised tumor are shown. NT: no tumor. Scale bars, 1 cm. (**C**) Representative H&E-stained images of excised tumors from the Z-GP-DAVLBH (2 μmol/kg)-treated groups are shown (n = 3). No tumor cells were observed in the tumor tissues. Scale bars, 1 mm.

Supplemental Figure 10. Z-GP-DAVLBH induces large MDA-MB-231 tumor xenografts regression. Mice bearing xenografts were received 2.0 μmol/kg i.v. injection of Z-GP-DAVLBH or saline containing 1% DMSO once every other day for 34 or 44 days, until the tumor volume reached approximately (**A**) 2,500 mm^3 (n = 5) or (**B**) 4,500 mm^3 (n = 5). The tumor growth curve is shown on the left in **B**, and the representative images of tumor regression induced by Z-GP-DAVLBH are shown on the right in **A** and **B**. No tumor cells are present in the tumor tissues. The error bar represents the SEM. Scale bar, 1 mm.

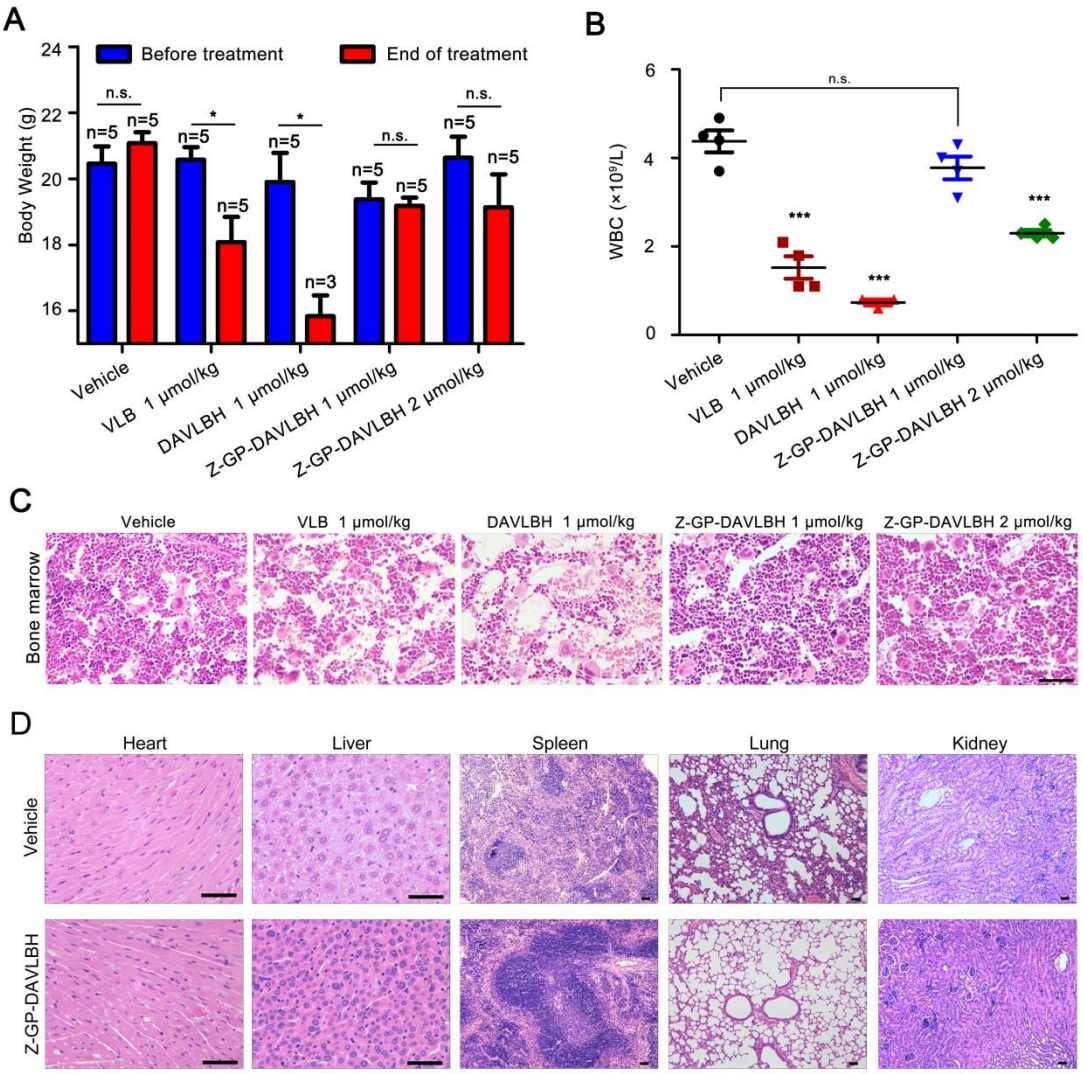

Supplemental Figure 11. Z-GP-DAVLBH shows reduced toxicity compared with DAVLBH. Blood samples, tissues and body weights were collected or calculated from mice bearing MDA-MB-231 tumor xenografts after seven i.v injections of the test compounds. (**A**) Mouse body weight was monitored before and after treatment. A significant loss of body weight was observed in the VLB and DAVLBH-treated group. (**B**) The white blood cells (WBCs) in each group of mice were counted at the end of treatment. The decrease in the number of WBCs in the mice treated with Z-GP-DAVLBH was relatively small compared with that in mice treated with VLB and DAVLBH. For **A** and **B,** the error bar represents the SEM. n.s.: no significant. **P*

< 0.05, ***P < 0.001 *versus* vehicle group, the data were analyzed by 2-tailed unpaired *t* test or 1-way ANOVA with Tukey's *post hoc* comparison, respectively. (**C**) Pathological examination of mouse bone marrow by H&E staining (n = 3). Myelosuppression was detectable in mice that received i.v injection of DAVLBH (1.0 μmol/kg) and Z-GP-DAVLBH (2.0 μmol/kg), as indicated by a decrease in the number of granulocytes and erythroid cells but not megakaryocytes. In contrast, mice that received Z-GP-DAVLBH at 1.0 μmol/kg showed no significant decrease in the three bone marrow cell groups. (**D**) The histopathological examination of major organs (heart, liver, spleen, lung and kidney) removed from vehicle and Z-GP-DAVLBH (2.0 μmol/kg) groups (n = 3). No significant pathological injury was observed in the Z-GP-DAVLBH (2.0 μmol/kg) group. Representative images are shown. Scale bars, 100 μm.

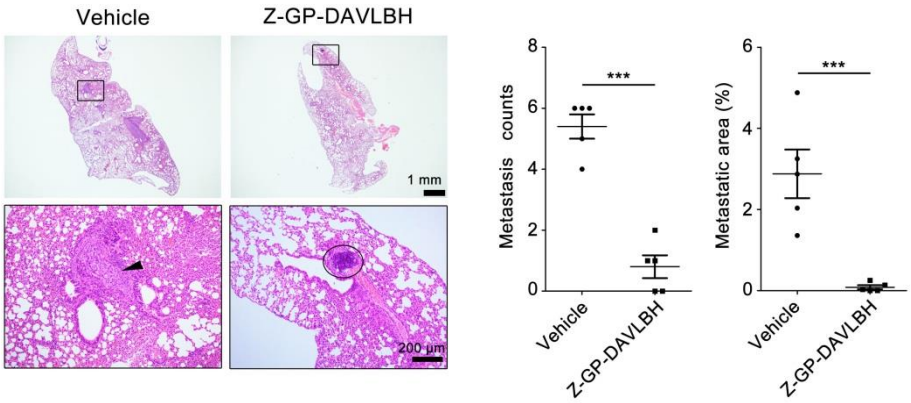

Supplemental Figure 12. Z-GP-DAVLBH inhibits tumor metastasis. Mice bearing MDA-MB-231 orthotopic xenografts were received i.v injection of 2.0 μmol/kg Z-GP-DAVLBH or saline containing 1% DMSO once every other day for 6 days. (**A**) H&E staining of lungs from the indicated experimental groups. The black arrowhead

marks the metastases, and the black ring marks the necrosis of the metastasis. (**B**) Quantification of the metastasis counts and metastatic area in lungs are shown (n = 5). The error bar represents the SEM. ***P < 0.001 *versus* vehicle group (2-tailed unpaired *t* test).

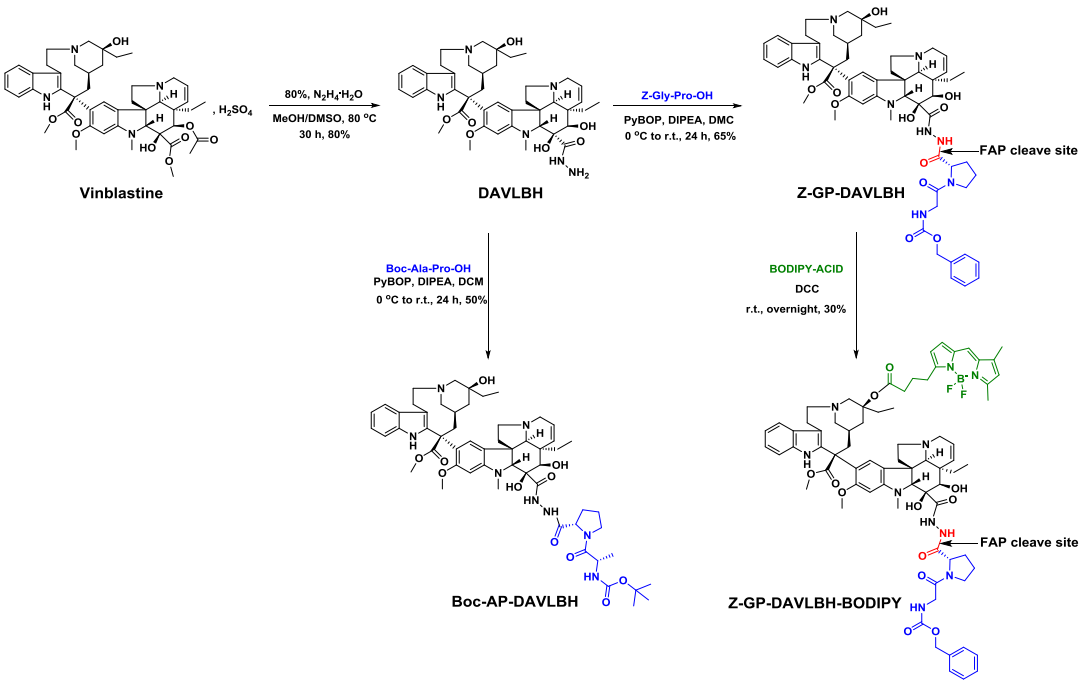

Supplemental Figure 13. Structures and synthetic schemes for DAVLBH, Z-GP-DAVLBH, Boc-AP-DAVLBH and Z-GP-DAVLBH-BODIPY.

Supplementary Table 1. Clinical characteristics of the resected cancers

Characteristics	Liver cancer patient	Breast cancer patient
Gender/Age (yr)	Male/60	Female/53
Date of diagnosis	7/2014	7/2014
Tumor type	Primary hepatocellular carcinoma, HBV+	Primary invasive ductal carcinoma, ER(+++), PR(++), HER2(-)
Clinical stage	pT3bN0M0 ⅢB	pT1N1M0 ⅡA
Treatment status	Post-operative chemotherapy	Post-operative chemotherapy
Clinical metastasis	None	Sentinel lymph node

Full unedited gels

Full unedited gel for Figure 2C

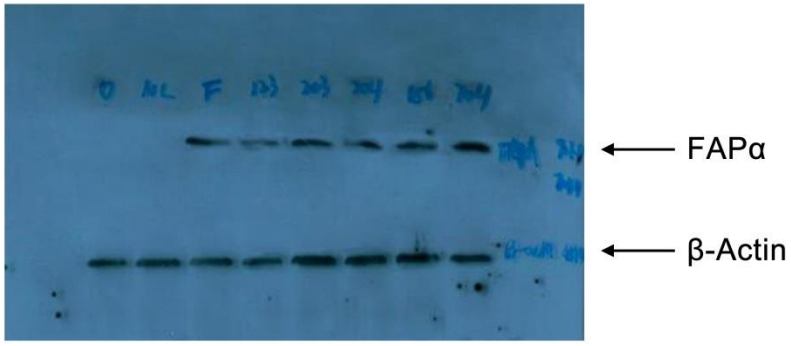

Full unedited gel for Figure 2E

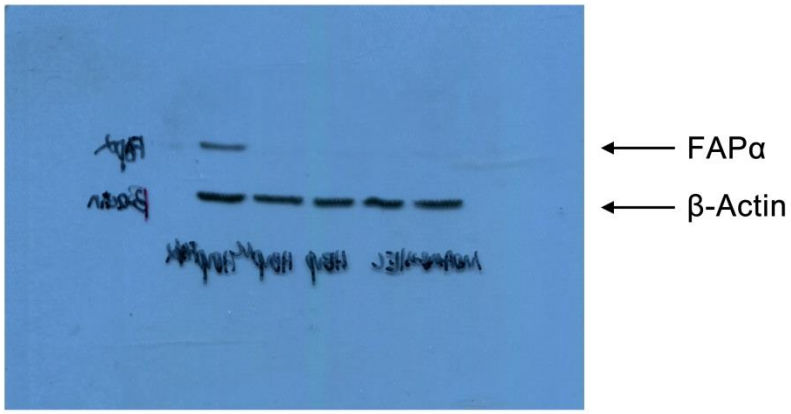

Full unedited gel for Supplemental Figure 7A